Thermal and chemical equilibration in relativistic heavy ion collisions

S. M. H. Wong

Laboratoire de Physique Théorique et Hautes Energies, Université de Paris XI, Bâtiment 211, F-91405 Orsay, France
and Fakultät für Physik, Universität Bielefeld, D-33501 Bielefeld, Germany

We investigate the thermalization and the chemical equilibration of a parton plasma created from Au+Au collision at LHC and RHIC energies starting from the early moment when the particle momentum distributions in the central region become for the first time isotropic due to longitudinal cooling. Using the relaxation time approximation for the collision terms in the Boltzmann equations for gluons and for quarks and the real collision terms constructed from the simplest QCD interactions, we show that the collision times have the right behavior for equilibration. The magnitude of the quark (antiquark) collision time remains bigger than the gluon collision time throughout the lifetime of the plasma so that gluons are equilibrating faster than quarks both chemically and kinetically. That is we have a two-stage equilibration scenario as has been pointed out already by Shuryak sometimes ago. Full kinetic equilibration is however slow and chemical equilibration cannot be completed before the onset of the deconfinement phase transition assumed to be at $T_c = 200$ MeV. By comparing the collision entropy density rates of the different processes, we show explicitly that inelastic processes, and *not* elastic processes as is commonly assumed, are dominant in the equilibration of the plasma and that gluon branching leads the other processes in entropy generation. We also show that, within perturbative QCD, processes with higher power in α_s need not be less important for the purpose of equilibration than those with lower power. The state of equilibration of the system has also a role to play. We compare our results with those of the parton cascade model. [S0556-2813(96)04211-2]

PACS number(s): 25.75.−q, 12.38.Bx, 12.38.Mh, 24.85.+p

I. INTRODUCTION

A goal of the future heavy ion collision experiments at the relativistic heavy ion collider (RHIC) at Brookhaven and at the large hadron collider (LHC) at CERN is to find the quark-gluon plasma. The primary aim is of course to show that quarks and gluons can indeed be freed from their hadronic ''prison'' and exist as individual entities in a hot plasma. Once this is realized, one can then turn to the diverse physics of such a new state of matter. One of these is the relation of the various thermodynamic variables to each other or in other words, the equation of state [1]. In order to probe this in experiments, an equilibrated quark-gluon plasma is required. In this work, we look at how far can one expect to have such a plasma in equilibrium. Because of the importance of this question, various different approaches have already been taken to address this issue. In particular, Shuryak [2] argued that equilibration of the plasma proceeds via two stages in the ''hot gluon scenario.'' First the equilibration of the gluons and then that of the quarks follows with a certain time delay. Thermal equilibration is quite short for gluon ≲ 1 fm with high initial temperature of 440 MeV at LHC and 340 MeV at RHIC. However, these estimates are based on thermal reaction rates for large and small angle scatterings and on the assumption that one scattering is sufficient to achieve isotropy of momentum distribution. As has been shown in [3] using a family of different power behaviors for the time dependence of the collision time, the assumption of one scattering is sufficient is a serious underestimate. With a larger number of scatterings, using the same arguments as in [2], the initial temperature will be lowered and the thermalization time will be increased. Also, we argue that estimates based on using the scattering rate alone is in-

correct, since in a medium, one must consider the difference of the scattering going forward and backward both weighed with suitable factors of particle distribution functions. Hence the process with the largest cross section is not necessarily the more important. However, we will show the two-stage equilibration scenario or in other words, gluons equilibrate much faster than quarks and antiquarks.

The other approach is the semiclassical parton cascade model (PCM) [4–6], which is based on solving a set of relativistic transport equations in full six-dimensional phase space using perturbative QCD calculation for the interactions, predicts an equilibration time of 2.4 fm/c for Au+Au collision at 200 GeV/nucleon. This approach, which uses a spatial and momentum distribution obtained from the measured nuclear structure functions for the partons as initial state, is very complicated. Due to the finite size of the colliding nuclei, it is hard to clearly identify thermalization in terms of the expected time-dependent behaviors of the various collective variables [5]. But by fitting the total particle rapidity and transverse momentum distributions of the defined central volume, roughly identical temperatures are obtained [5] and hence the claim of thermalization. However, in terms of the same distributions of the individual parton components, this becomes less obvious to be the case [6]. As was stated in [6], the momentum distributions are not perfect exponentials and therefore there is no complete thermalization in any case.

We will look at this problem of equilibration using a much simpler approach which is based on the Boltzmann equation and the relaxation time approximation for the collision terms. Initially used by Baym [7] to study thermal equilibration and has subsequently been used in the study of various related problems [8–11]. The conclusion of these

works is, in general, if the collision time θ which enters in the relaxation approximation, grows less fast than the expansion time τ, then thermal equilibration can be achieved eventually. In the case of the quark-gluon plasma, it is not sufficient to know that equilibration will be achieved eventually because the plasma has not an infinite lifetime in which to equilibrate. We would like to know how far can it equilibrate before the phase transition. To answer such a question, we will use both the relaxation time approximation and the interactions obtained from perturbative QCD for the collision terms to determine θ. This approach has been used previously to study both thermal and chemical equilibration in a gluon plasma [11] where it was found that with the initial conditions obtained from HIJING results, the gluon plasma had not quite enough time to completely equilibrate. In the present case of a quark and gluon parton plasma, quarks and gluons are treated as different particle species rather than as generic partons and so they have different time-dependent collision times. As a result, they approach equilibrium at different rates and towards different target temperatures. The latters will converge only at large times. It follows that the system can only equilibrate as one single system at large times. This lends support to the two-stage equilibration scenario [2].

In an expanding system, particles are not in equilibrium early on because interactions are not fast enough to maintain this so they are most likely to start off free streaming in the beam direction [10,12]. Thermalization will be seen as the gradual reduction of this free streaming effect as interactions gain pace and momentum transfer processes are put into action to bring the particle momenta into an isotropic distribution. The present approach takes into account of these effects.

As in the previous work [11], isotropic momentaneously thermalized initial conditions are used at both RHIC and LHC energies. These are obtained from HIJING results after allowing the partons to free stream until the momentum distribution becomes isotropic for the first time [13–15]. From then on, interactions are turned on but the distribution becomes anisotropic again due to the tendency of the particles to continue to free stream. It is the role of interactions to reduce this and to progressively bring the distributions into the equilibrium forms. We have shown that, surprisingly, kinetic equilibration in a pure gluon plasma is driven mainly by gluon multiplication and not gluon-gluon elastic scattering. In this paper, we include quarks and antiquarks and consider the equilibration of a proper QCD plasma. We explicitly break down the equilibration process into each of its contributing elements and show which interactions are more important and hence uncover the dominant processes for equilibration. In fact, our result is *inelastic* interactions are most important for this purpose both for quarks and for gluons.

Our paper is organized as follows. In Sec. II, we describe the Boltzmann equations with the relaxation time approximation for two particle species. In Sec. III, the time-dependent behavior of the collision times, θ's, necessary for equilibration will be analyzed and extracted. The particle interactions entering into the collision terms and details of their calculations will be explained in Sec. IV. Initial conditions used will be given in Sec. V and lastly the results of the evolution of

the plasma will be shown and discussed in Sec. VI. We finish with a brief discussion of the differences with the results of PCM.

II. RELAXATION TIME APPROXIMATION FOR TWO PARTICLE SPECIES

In the absence of relativistic quantum transport theory derived from first principle of QCD [16–22], we base our approach on Boltzmann equation with both the relaxation time approximation for the collision terms and the real collision terms obtained from perturbative QCD. Treating quarks and gluons on different footings, we write down the Boltzmann equations

$$\frac{\partial f_i}{\partial t} + \mathbf{v}_{\mathbf{p}i} \cdot \frac{\partial f_i}{\partial \mathbf{r}} = C_i(\mathbf{p},\mathbf{r},t) \tag{1}$$

where f_i is the one-particle distribution and C_i stands for the collision terms and includes all the relevant interactions for particle species i and $i = g,q,\bar{q}$. Concentrating in the central region of the collision where we assumed to be spatially homogeneous, baryon free and boost invariant in the z direction (beam direction) so that $f_q = f_{\bar{q}}$ and $f_i = f_i(\mathbf{p}_\perp, \mathbf{p}'_z, \tau)$ where $p'_z = \gamma(p_z - up)$ with $\gamma = 1/\sqrt{1-u^2}$ and $u = z/t$ is the boosted particle z-momentum component and $\tau = \sqrt{t^2 - z^2}$ is the proper time. Following Baym [7], the Boltzmann equation can be rewritten as

$$\left. \frac{\partial f_i}{\partial \tau} \right|_{p_z \tau} = C_i(p_\perp, p_z, \tau) \tag{2}$$

in the central region. Using the relaxation time approximation

$$C_i(p_\perp, p_z, \tau) = -\frac{f_i(p_\perp, p_z, \tau) - f_{\mathrm{eq}i}(p_\perp, p_z, \tau)}{\theta_i(\tau)} \tag{3}$$

where $f_{\mathrm{eq}i}$ is the equilibrium distribution and θ_i is the collision time for species i, this allows us to write down a solution to Eq. (2),

$$f_i(\mathbf{p},\tau) = f_{0i}(p_\perp, p_z \tau/\tau_0) e^{-x_i}$$
$$+ \int_0^{x_i} dx'_i e^{x'_i - x_i} f_{\mathrm{eq}i}(\sqrt{p_\perp^2 + (p_z \tau/\tau')^2}, T_{\mathrm{eq}i}(\tau')),$$
$$\tag{4}$$

where

$$f_{0i}(p_\perp, p_z \tau/\tau_0) = [\exp(\sqrt{p_\perp^2 + (p_z \tau/\tau_0)^2}/T_0)/l_{0i} \mp 1]^{-1}, \tag{5}$$

is the solution to Eq. (2) when $C = 0$ which is also the distribution function at the initial isotropic time τ_0, with initial fugacities l_{0i} and temperature T_0. It is of such a form because of the assumption of momentaneously thermalized initial condition. The functions $x_i(\tau)$'s, given by

$$x_i(\tau) = \int_{\tau_0}^{\tau} d\tau'/\theta_i(\tau'), \tag{6}$$

play the same role as θ_i's in the sense that their time-dependent behaviors control thermalization. T_{eqi}, that appears in f_{eqi}, is the time-dependent momentane target equilibrium temperature for the i particle species. The two terms of equation Eq. (4) can be thought of, up to exponential factor, as the free streaming (first term) and equilibrium term (second term). Whether species i equilibrates or not depends on which of the two terms dominates.

In the present case of two species, the energy conservation equations are, in terms of the equilibrium ideal gas energy densities $\epsilon_{eqg} = a_2 T^4_{eqg}$, $\epsilon_{eqq} = n_f b_2 T^4_{eqg}$, $a_2 = 8\pi^2/15$, $b_2 = 7\pi^2/40$ and n_f is the number of quark flavors,

$$\frac{d\epsilon_i}{d\tau} + \frac{\epsilon_i + p_{Li}}{\tau} = -\frac{\epsilon_i - \epsilon_{eqi}}{\theta_i} \qquad (7)$$

and

$$\frac{d\epsilon_{tot}}{d\tau} + \frac{\epsilon_{tot} + p_{Ltot}}{\tau} = 0, \qquad (8)$$

where $\epsilon_{tot} = \Sigma_i \epsilon_i$ and $p_{Ltot} = \Sigma_i p_{Li}$, or in other words

$$\sum_i \frac{\epsilon_i - \epsilon_{eqi}}{\theta_i} = 0. \qquad (9)$$

The above equation only expresses the fact that energy loss of one species must be the gain of the other. The transport equations of the different particle species are therefore coupled as they should be. The longitudinal and transverse pressures are defined as before

$$p_{L,Ti}(\tau) = \nu_i \int \frac{d^3\mathbf{p}}{(2\pi)^3} \frac{p^2_{z,x}}{p} f_i(p_\perp, p_z, \tau), \qquad (10)$$

with $\nu_g = 2 \times 8 = 16$ and $\nu_q = 2 \times 3 \times n_f = 6 n_f$, the multiplicities of gluons and quarks, respectively.

Here the equilibrium target temperatures T_{eqg} and T_{eqq} cannot be the same in general since, as we will see in Sec. VI, $\theta_g \neq \theta_q = \theta_{\bar{q}}$. Therefore gluons and quarks will approach equilibrium at different rates. Note that energy conservation here *does not* mean

$$\epsilon_g + 2\epsilon_q = \epsilon_{eqg} + 2\epsilon_{eqq} \qquad (11)$$

since $\theta_g < \theta_q$ always, at least at small times, so gluon energy density ϵ_g will approach ϵ_{eqg} faster than ϵ_q approaches ϵ_{eqq} so the two equilibrium energy densities should not be considered to be those which can coexist at the same moment. This can only be true at large τ when $T_{eqg} \simeq T_{eqq}$ and $\theta_g \simeq \theta_q$. If Eq. (11) were true, the condition for energy conservation Eq. (9) could not hold when $\theta_g \neq \theta_q$. Since our QCD plasma is a dynamical system under one-dimensional expansion as well as particle production, the target temperatures T_{eqg} and T_{eqq} must be changing continuously and must approach each other at large times before the gluon and quark (antiquark) subsystems can merge into one system and exist at one single temperature. Likewise, we believe θ_g and θ_q should also converge to a single value at large times, unfortunately, this will take too long to happen in the evolution of our plasma although we can be sure that both θ_g and

θ_q increase less fast than the expansion time τ near the end of the evolution, a condition which, as has already been stated in the Introduction and we will see again in Sec. III, is necessary for thermalization.

III. CONDITIONS ON θ_g AND θ_q FOR THERMALIZATION

Before considering the evolution of the QCD plasma under real interactions, we can deduce analytically, using Eq. (2) and Eq. (4), the conditions on the θ_i's under which the plasma will come to kinetic equilibrium. Multiplying Eq. (4) by particle energy and integrating over momentum, we have the equations for the ϵ_i's. Further manipulating these gives

$$\int_0^{x_i} dx_i' e^{x_i'} \left\{ \tau' h(\tau'/\tau)[\epsilon_{eqi}(\tau') - \epsilon_i(\tau')] \right.$$
$$\left. - \frac{d}{dx_i'} [\tau' h(\tau'/\tau)\epsilon_i(\tau')] \right\} = 0, \qquad (12)$$

where

$$h(r) = \int_0^1 dy \sqrt{1 - y^2(1-r^2)} = \frac{1}{2}\left(r + \frac{\sin^{-1}\sqrt{1-r^2}}{\sqrt{1-r^2}} \right) \qquad (13)$$

and $x_i' = x_i(\tau')$. Supposing as $\tau \to \infty$, $x_g \to \infty$, and $x_q \to \infty$ then the integrand in Eq. (12) will be weighed by the $\tau' \to \infty$ or large x_i' limit. It follows that the term within braces in Eq. (12) must be zero at large τ' so using $h'(r)|_{r=1} = 1/3$, we have

$$\frac{d\epsilon_i}{d\tau} + \frac{4}{3}\frac{\epsilon_i}{\tau} = -\frac{\epsilon_i - \epsilon_{eqi}}{\theta_i}. \qquad (14)$$

This means each species will undergo near hydrodynamic expansion at large τ modified by energy lost to or energy gained from the other species. The latter should be small at such times. Summing Eq. (14) over species, we obtain the energy conservation equation for a system undergoing hydrodynamic expansion

$$\frac{d\epsilon_{tot}}{d\tau} + \frac{4}{3}\frac{\epsilon_{tot}}{\tau} = 0, \qquad (15)$$

with $p_{Ltot} = \epsilon_{tot}/3$.

If one θ_i is such that the corresponding $x_i \to x_{i\infty} < \infty$ as $\tau \to \infty$ then hydrodynamic expansion does not apply to that species since we have

$$\frac{d(\epsilon_i \tau)}{d\tau} = -\frac{(\epsilon_i - \epsilon_{eqi})\tau}{\theta_i} - p_{Li}, \qquad (16)$$

where now $p_{Li} \neq \epsilon_i/3$, so kinetic equilibrium is not established. The right-hand side (rhs) of Eq. (16) is negative if these particles are losing energy or gaining energy at a rate less than p_{Li}/τ at large τ. Therefore $\epsilon_i \tau$ must decrease towards a nonzero asymptotic value $(\epsilon_i \tau)_\infty$, since $x_{i\infty} < \infty \Rightarrow \epsilon_i \tau > 0$ always, which results in a free streaming final state for these particles

$$\epsilon_i(\tau \rightarrow \infty) \sim (\epsilon_i \tau)_\infty / \tau. \qquad (17)$$

A similar free streaming final state will be reached if the rate of gaining energy is larger than p_{Li}/τ at large τ. In this case, although $\epsilon_i \tau$ is increasing, the ϵ_j of the other particle species with $x_j \rightarrow \infty$ as $\tau \rightarrow \infty$ will be close to ϵ_{eqj} and so the energy transfer will be very small. One can deduce that as $\tau \rightarrow \infty$

$$1 \gg \frac{\epsilon_{eqi} - \epsilon_i}{\theta_i} \rightarrow 0 > \frac{p_{Li}}{\tau} \Rightarrow \frac{d(\epsilon_i \tau)}{d\tau} \rightarrow 0, \qquad (18)$$

hence $\epsilon_i \tau \rightarrow (\epsilon_i \tau)_\infty$. That is $\epsilon_i \tau$ now increases towards some asymptotic value instead of decreasing towards one as in the previous case. But it ends up with a free streaming final state nevertheless. We do not consider the case where the relative rate $(\epsilon_{eqi} - \epsilon_i)\tau / \theta_i p_{Li}$ oscillates about one at large τ except to say that on the average $d(\epsilon_i \tau)/d\tau \sim 0$ and so an average free streaming final state is likely.

The last possibility where $x_i \rightarrow x_{i\infty} < \infty$ as $\tau \rightarrow \infty$ for both particle species, Eq. (16) applies to both. Barring the case of the oscillating relative rate, one particle species must lose energy and so by the above argument, a free streaming final state results. For the remaining particle species, it does not matter whether $d(\epsilon_i \tau)/d\tau$ is or is not positive at large τ, these particles will also be in a free streaming final state. If the rate is negative, then the same argument that leads to Eq. (17) applies. If it is positive, since the species that is losing energy is approaching free streaming so the energy transfer must go to zero. Then we are back to Eq. (18).

The conclusions are therefore, depending on the time-dependent behaviors of θ_g and θ_q, as follows.

(1) $x_g \rightarrow \infty$ and $x_q \rightarrow \infty$ as $\tau \rightarrow \infty$ are required for the whole system to completely thermalize.

(2) $x_g \rightarrow \infty$ and $x_q \rightarrow x_{q\infty} < \infty$ or $x_q \rightarrow \infty$ and $x_g \rightarrow x_{g\infty} < \infty$ as $\tau \rightarrow \infty$ imply that only the species with $x_i \rightarrow \infty$ will thermalize, the other species will not equilibrate but free streams at the end. The system will end up somewhere between free streaming and hydrodynamic expansion.

(3) Both $x_g \rightarrow x_{g\infty} < \infty$ and $x_q \rightarrow x_{q\infty} < \infty$ as $\tau \rightarrow \infty$ then the whole system will end up in a free streaming final state.

One can understand these x_i behaviors in terms of θ_i's by assuming simple power τ dependence for the latters. One finds that θ_i's must all grow slower than τ for the whole system to achieve thermalization. If either one or more grow faster then a mixed or a complete free streaming final state results.

IV. PARTICLE INTERACTION–COLLISION TERMS

To investigate the evolution of a proper QCD plasma, we consider the following simplest interactions at the tree level:

$$gg \leftrightarrow ggg, \quad gg \leftrightarrow gg, \qquad (19)$$

$$gg \leftrightarrow q\bar{q}, \quad gq \leftrightarrow gq, \quad g\bar{q} \leftrightarrow g\bar{q}, \qquad (20)$$

$$q\bar{q} \leftrightarrow q\bar{q}, \quad qq \leftrightarrow qq, \quad \overline{qq} \leftrightarrow \overline{qq}. \qquad (21)$$

As in [13–15], we include only the leading inelastic processes, i.e., the first interaction of Eq. (19) and Eq. (20).[1] We will return to this point later on in Sec. VI.

In the solutions Eq. (4) to the Boltzmann equations Eq. (2), there are two time-dependent unknown parameters θ_i and T_{eqi} for each species which very much control the particle distributions. To determine them, we need two equations each for gluons and for quarks. In order to show the relative importance of the various interactions Eqs. (19), (20), and (21) in equilibration, we find these time-dependent parameters by constructing equations from the rates of energy density transfer between quarks (antiquarks) and gluons and the collision entropy density rates.

From Eqs. (2), (3), and (4), the energy density transfer rates are

$$\frac{d\epsilon_i}{d\tau} + \frac{\epsilon_i + p_{Li}}{\tau} = -\frac{\epsilon_i - \epsilon_{eqi}}{\theta_i}$$

$$= \nu_i \int \frac{d^3\mathbf{p}}{(2\pi)^3} p\, C_i(p_\perp, p_z, \tau) = \mathcal{E}_i, \quad (22)$$

where $\mathcal{E}_i$ is the energy gain or loss of species i per unit time per unit volume. As stated in Sec. II, $\mathcal{E}_i$'s must obey $\Sigma_i \mathcal{E}_i = 0$ for energy conservation.

The other equations, the collision entropy rates can be deduced from the explicit expression of the entropy density in terms of particle distribution function [23]

$$s_i(\tau) = -\nu_i \int \frac{d^3\mathbf{p}}{(2\pi)^3} \{f_i(\mathbf{p}, \tau) \ln f_i(\mathbf{p}, \tau)$$

$$\mp (1 \pm f_i(\mathbf{p}, \tau)) \ln(1 \pm f_i(\mathbf{p}, \tau))\}, \qquad (23)$$

where the different signs are for bosons and fermions, respectively. They are, using again Eqs. (2), (3), and (4),

$$\left(\frac{ds_i}{d\tau}\right)_{coll} = -\nu_i \int \frac{d^3\mathbf{p}}{(2\pi)^3} \left(\frac{\partial f_i}{\partial \tau}\right)_{coll} \ln\left(\frac{f_i}{1 \pm f_i}\right) \qquad (24)$$

$$= -\nu_i \int \frac{d^3\mathbf{p}}{(2\pi)^3} C_i(p_\perp, p_z, \tau) \ln\left(\frac{f_i}{1 \pm f_i}\right) \qquad (25)$$

$$= \nu_i \int \frac{d^3\mathbf{p}}{(2\pi)^3} \frac{f_i - f_{eqi}}{\theta_i} \ln\left(\frac{f_i}{1 \pm f_i}\right). \qquad (26)$$

By using the explicit expression for the collision terms C_i's constructed from the interactions Eqs. (19), (20), and (21) within perturbative QCD, Eqs. (22), (25), and (26) allow us to solve for θ_i's and T_{eqi}'s.

The gluon multiplication contribution to C_g is constructed from the infrared regularized Bertsch and Gunion formula [24] for the amplitude with partial incorporation of Landau-Pomeranchuk-Migdal suppression (LPM) for gluon emission

---

[1] The first one of Eq. (21) could also be inelastic but here we give the same chemical potential to all the fermions so we do not consider quark-antiquark annihilations into different flavors as inelastic for our purpose.

and absorption [13,25–27] as in the previous work [11]. The explicit form of the gluon multiplication collision term and a discussion of the problem regarding how to incorporate the LPM effect correctly can be found there also. The remaining binary interaction contributions to C_i for particle 1 is, as usual, given by

$$
\begin{aligned}
C_{i1}^{\text{binary}} = -\sum_{\mathcal{P}_i} \frac{S_{\mathcal{P}_i}\nu_2}{2p_1^0} \prod_{j=2}^4 \frac{d^3\mathbf{p}_j}{(2\pi)^3 2p_j^0} \\
\times (2\pi)^4 \delta^4(p_1+p_2-p_3-p_4)|\mathcal{M}_{1+2\to3+4}^{\mathcal{P}_i}|^2 \\
\times [f_1 f_2(1\pm f_3)(1\pm f_4) - f_3 f_4(1\pm f_1)(1\pm f_2)],
\end{aligned}
$$
(27)

where the $\mathcal{P}_i$ runs over all the binary processes in Eqs. (19), (20), and (21) which involve species i, $|\mathcal{M}^{\mathcal{P}_i}|^2$ is the sum over final states and averaged over initial state squared matrix element, $S_{\mathcal{P}_i}$ is a symmetry factor for any identical particles in the final states for the process $\mathcal{P}_i$ and ν_2 is the multiplicity of particle 2.

We take $|\mathcal{M}^{\mathcal{P}_i}|^2$'s from [28] and infrared regularized them using either the Debye mass m_D^2 for gluons or the quark medium mass m_q^2 for quarks to cut off any infrared divergence. These masses are now time-dependent quantities in a nonequilibrium environment. With nonisotropic momentum distribution, both the Debye mass [29,30] and the gluon medium mass, m_g^2, are directional dependent. This is, however, not the case for the quark medium mass, m_q^2, which remains directional independent as in equilibrium. The directional dependence arises out of the cancellations between identical type of distribution functions similar to those one finds in the derivation of hard thermal loops [31,32]. To keep things simple, we removed the directional dependence from m_D^2 and use, for SU($N=3$), to leading order in α_s,

$$
m_D^2(\tau) = -8\pi\alpha_s \int \frac{d^3\mathbf{p}}{(2\pi)^3} \frac{\partial}{\partial|\mathbf{p}|}(Nf_g + n_f f_q). \quad (28)
$$

For the quark medium mass, to the same order, we use

$$
m_q^2(\tau) = 4\pi\alpha_s \left(\frac{N^2-1}{2N}\right) \int \frac{d^3\mathbf{p}}{(2\pi)^3} \frac{1}{|\mathbf{p}|}(f_g + f_q), \quad (29)
$$

which is just the equilibrium expression but with nonequilibrium distribution functions.

With these masses, we regularize the squared matrix elements by hand and inserting the masses as follows:

$$
|\mathcal{M}_{gg\to gg}|^2 = \frac{9g^2}{2}\left(3 - \frac{ut}{(s+m_D^2)^2} - \frac{us}{(t-m_D^2)^2} - \frac{st}{(u-m_D^2)^2}\right),
$$
(30)

$$
|\mathcal{M}_{gg\to q\bar{q}}|^2 = \frac{g^2}{6}\left(\frac{t}{(u-m_q^2)} + \frac{u}{(t-m_q^2)}\right) - \frac{3}{8}\frac{u^2+t^2}{(s+4m_q^2)^2},
$$
(31)

$$
|\mathcal{M}_{gq\to gq}|^2 = |\mathcal{M}_{g\bar{q}\to g\bar{q}}|^2
$$
$$
= g^2\left[1 - \frac{2us}{(t-m_D^2)^2} - \frac{4}{9}\left(\frac{u}{(s+m_q^2)} + \frac{s}{(u-m_q^2)}\right)\right],
$$
(32)

$$
|\mathcal{M}_{qq\to qq}|^2 = |\mathcal{M}_{\bar{q}\bar{q}\to\bar{q}\bar{q}}|^2
$$
$$
= \frac{2g^2}{9}\left(\frac{2(s^2+t^2)}{(u-m_D^2)^2} + \delta_{12}\frac{2(u^2+s^2)}{(t-m_D^2)^2}\right.
$$
$$
\left. - \delta_{12}\frac{4}{3}\frac{s^2}{(t-m_D^2)(u-m_D^2)}\right),
$$
(33)

$$
|\mathcal{M}_{q\bar{q}\to q\bar{q}}|^2 = \frac{2g^2}{9}\left(\delta_{13}\delta_{24}\frac{2(s^2+t^2)}{(u-m_D^2)^2} + \delta_{12}\delta_{34}\frac{2(t^2+u^2)}{(s+4m_q^2)^2}\right.
$$
$$
\left. - \delta_{12}\delta_{13}\delta_{34}\frac{4}{3}\frac{t^2}{(u-m_D^2)(s+4m_q^2)}\right),
$$
(34)

where the δ_{ij} signifies that the i and j quark or antiquark must be of the same flavor. This regularization amounts to screening spacelike and timelike infrared gluons by m_D^2 and $4m_q^2$, respectively and infrared quarks by m_q^2. We stress that this regularization is done in a very simple manner and with the right order of magnitude for the cutoffs. Its aim is to get some estimates to the collision rates without involving too much with the exact and necessarily complicated momentum dependent form of the true infrared screening self-energies in an out-of-equilibrium plasma when their infrared screening effects should be in action. They should be the extension of the two-point gluon and quark hard thermal loops [31–35] to a nonthermalized environment.

We should mention here that the choice of the pair of equations for solving the two time-dependent unknowns θ_i and $T_{\text{eq}i}$ for each particle species is not unique. One can equally use, for example, the rate equations for the particle number density instead of the collision entropy density. With these other choices, the values of the different quantities are shifted somewhat due to the way that the initial conditions are extracted but there is no qualitative different in the result. Our present choice has the distinct advantage that we can explicitly compare the different processes using the collision entropy density rates. This will become clear when we show the results in Sec. VI.

V. INITIAL CONDITIONS

To start the evolution, we use the same initial conditions for the gluon plasma as before [11] based on HIJING result for Au+Au collision. The initial conditions for the quarks (antiquarks) are obtained by taking a ratio of 0.14 for the number of initial quark (antiquark) to the initial total number of partons as done in [13–15]. The initial conditions are shown in Table I. One sees that the initial quark collision times are long compared to those of the gluons both at RHIC and LHC. Especially at RHIC, the quark collision time is exceedingly long and so these particles are essentially free streaming initially. Taking these numbers as guides to how fast each particle species is going to equilibrate, we can be

TABLE I. Initial conditions for the evolution of a QCD plasma created in Au+Au collision at RHIC and at LHC.

| | Initial conditions | |
	RHIC	LHC
τ_0 (fm/c)	0.70	0.50
T_0 (GeV)	0.50	0.74
ϵ_{0g} (GeV/fm^3)	3.20	40.00
ϵ_{0q} (GeV/fm^3)	0.63	7.83
n_{0g} (fm^{-3})	2.15	18.00
n_{0q} (fm^{-3})	0.42	3.53
l_{0g}	0.08	0.21
l_{0q}	0.017	0.044
θ_{0g} (fm/c)	2.18	0.73
θ_{0q} (fm/c)	239.72	30.92

sure already of a two-stage equilibration scenario [2].

Using the standard initial picture of heavy ion collisions as before, our evolution is started when the momentum distribution in the central region of the collision becomes, for the first time, isotropic due to longitudinal cooling. The subsequent development is determined by the interactions Eqs. (19), (20), and (21). In the case of a pure gluon plasma [11], it is clear that interactions bring the system towards equilibrium and not towards some free streaming final state which is a possible alternative as can be inferred from the analysis in Sec. III. That is the interactions dominate over the expansion. In the present situation, we will see that the same can certainly be said for the gluons and for the quarks at LHC but at RHIC, it is less clear for the latters. The equilibration time for quarks is at least several times longer than that of the gluons.

Details for the procedure of the computation can be found in [11]. The values for the numerical parameters are the same and in addition, we use $n_f = 2.5$ to take into account of the reduced phase space of strange quark. All time integrations are discretized and the rates are obtained at each time step necessary for forming the two pairs of equations Eqs. (22), (25), and (26). One then solves the two equilibrium temperatures T_{eqg} and T_{eqq} from two fourth degree polynomials, one for each of the temperatures. From these solutions, θ_g and θ_q are obtained and everything is then fed back into the equations for the next time step.

VI. EQUILIBRATION OF THE QCD PLASMA

We show the results of our computation in this section. They show clearly the collision times θ_g and θ_q hold the keys to equilibration as have been analyzed in Sec. III. We will see shortly that as a result of the disparity between their magnitudes at finite values of τ, the equilibration of quarks and antiquarks lags behind that of the gluons both chemically and kinetically. We will also identify the dominant processes responsible for equilibration. They are *not* the commonly assumed elastic scattering processes as already mentioned in the Introduction.

When dealing with two particle species, one has several choices as to when should the evolution be stopped. We choose to do this when both the quark and the gluon temperature estimates drop to 200 MeV. For gluons, this esti-
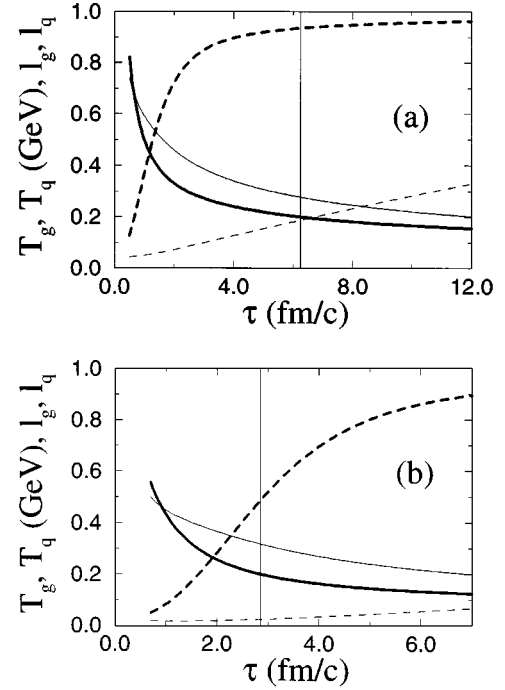

FIG. 1. The time dependence of the estimated temperatures for quarks and for gluons and their fugacities at (a) LHC and (b) RHIC. The solid lines are the estimated temperatures T_g (thick line) and T_q. The dashed lines are the fugacities l_g (thick line) and l_q. Gluon chemical equilibration is much faster than that of the quarks. The curves are stopped when all the temperature estimates drop to 200 MeV. The vertical line indicates when the gluon temperature reaches this value.

mate is obtained by the near equilibrium energy and number density expression

$$\epsilon_g = a_2 l_g T_g^4 \quad \text{and} \quad n_g = a_1 l_g T_g^3, \qquad (35)$$

which are valid when the fugacity l_g is near 1.0, i.e., when the distribution functions can be approximated by $f_g(\mathbf{p}, l_g, \tau) = l_g f_g(\mathbf{p}, l_g = 1, \tau)$. For quarks and antiquarks, we cannot do the same as l_q has not time to rise above 0.5 so instead, the temperature is estimated from the same quantities in kinetic equilibrium but at small values of l_q

$$\epsilon_q = 3\nu_q l_q T_q^4/\pi^2 \quad \text{and} \quad n_q = \nu_q l_q T_q^3/\pi^2. \qquad (36)$$

These estimates are plotted in Fig. 1. The vertical line marks the point when the gluon temperature estimate (thick solid line) drops to 200 MeV. At this point, $\tau \sim 6.25$ fm/c, the fugacity (thick dashed line) is $l_g \sim 0.935$ at LHC and is $l_g \sim 0.487$ at $\tau \sim 2.85$ fm/c at RHIC. On the same plots, the quark temperature (solid line) drops at a slower rate and the fermionic fugacity (dashed line) is also increasing much slower given the less favorable initial conditions and initially much slower quark-antiquark pair creation than gluon multiplication rate. In the end, the fermions are not too well chemically equilibrated and in fact, are still quite far away from 1.0. This is especially bad at RHIC. We note that comparing to [13–15], in our case, gluons chemically equilibrate faster but quarks are slower.

Unlike chemical equilibration, kinetic equilibration has no simple indicators like the fugacities that can allow itself to be simply quantified. One has to, instead, use the anisotropy of momentum distribution as well as various reaction rates to get an idea of the degree of kinetic equilibration. The former can be deduced from the ratios of the longitudinal pressure and a third of the energy density to the transverse pressure, p_L/p_T and $\epsilon/3p_T$, respectively. Whereas from the elastic scattering rates, one can deduce roughly how close the distribution functions are to their equilibrium forms by virtue of the fact that in local kinetic equilibrium, these rates are zero. The pressure ratios p_L/p_T (solid line) and $\epsilon/3p_T$ (dashed line) are plotted in Figs. 2(a) and (a′) for gluons, (b) and (b′) for quarks, and (c) and (c′) for the total sum. These ratios are indeed approaching 1.0, the expected value after thermalization, but at different rates. Gluons are clearly equilibrating much faster than quarks which proceed rather slowly.

To show that these behaviors, although slow, are indeed the signs of equilibration and that the plasma is not approaching some free streaming final states, we can work out what their behaviors should be in the latter case by taking the extreme and let $\theta_i \to \infty$. From Eq. (10), as $\tau \to \infty$,

$$\left.\begin{array}{l} p_L \to \pi\tau_0^3\epsilon_0/4\tau^3 \\ p_T \to \pi\tau_0\epsilon_0/8\tau \\ \epsilon \to \pi\tau_0\epsilon_0/4\tau \end{array}\right\} \Rightarrow \begin{cases} p_L/p_T \to 2\tau_0^2/\tau^2 \to 0 \\ \epsilon/3p_T \to 2/3 \end{cases} \quad (37)$$

where ϵ_0 is the initial energy density and the above ratios are valid for both quarks and gluons in this extreme. Therefore in the free streaming case, the first ratio should approach zero and the second should approach 2/3. These are clearly not what we see in our plots.

To best get an idea of how close the distribution functions are to the equilibrium forms, the gg and qq or $\overline{qq}$ elastic scattering processes are ideal for this. These are shown in Fig. 6 and Fig. 7(b) for gluon and Fig. 8 and Fig. 9(c) for quark. Note that the peaks of these collision entropy rates coincide with the corresponding mininum points of the pressure ratios. As expected, the rates maximize at maximum anisotropy in momentum distribution. They all rise rapidly from zero at τ_0 when the interactions are turned on. The subsequent return to zero or the approach of the distribution functions to their equilibrium forms are, however, much less rapid. They only do so progressively as can be deduced already from the pressure ratio plots.

Having shown chemical and kinetic equilibrations separately, we present now the actual approach of the collective variables towards the equilibrium values. Since we are more interested in the behavior of their time dependence than their absolute magnitudes, we multiplied them by their expected time dependence and scaled these by taking a guess at the corresponding asymptotic values from the tendency of the curves. The results are plotted in Fig. 3. They are $\epsilon_i\tau^{4/3}/\epsilon_{si}\tau_{si}^{4/3}$, $n_i\tau/n_{si}\tau_{si}$ and $s_i\tau/s_{si}\tau_{si}$ in the figures (a) and (a′), (b) and (b′), and (c) and (c′), respectively. All these should be nearly constant with respect to time at large τ. The solid lines are for gluons and the dashed ones are for quarks. They showed that the curves do behave in such a way for the eventual constant behavior. This feature is much clearer at LHC than at RHIC which only reconfirms the previously
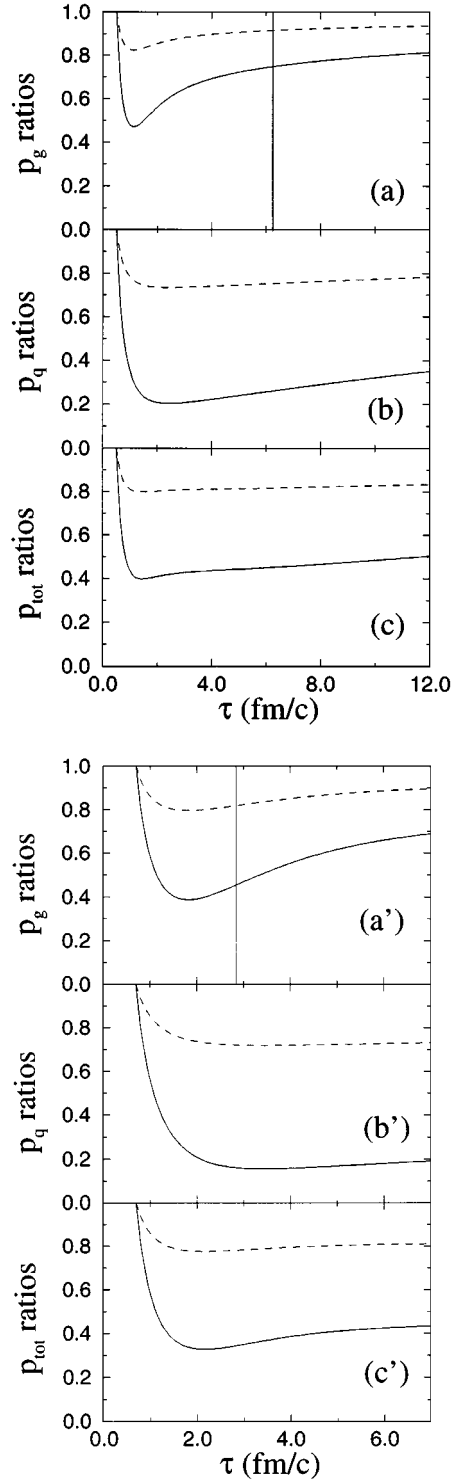

FIG. 2. The ratios of the longitudinal pressure (solid line) and a third of the energy density (dashed line) to the transverse pressure, p_L/p_T and $\epsilon/3p_T$ respectively for (a) gluons, (b) quarks, and (c) the total sum at LHC. Graphs (a′), (b′), and (c′) are the same at RHIC.

deduced result of faster equilibration at LHC than at RHIC. Note that for gluons, the quantities are approaching the corresponding asymptotic values from above, whereas for quarks, this approach is from below. This is because of the simple reason that there is a net conversion of gluons into quark-antiquark pairs via $gg \leftrightarrow q\overline{q}$. The corresponding colli-
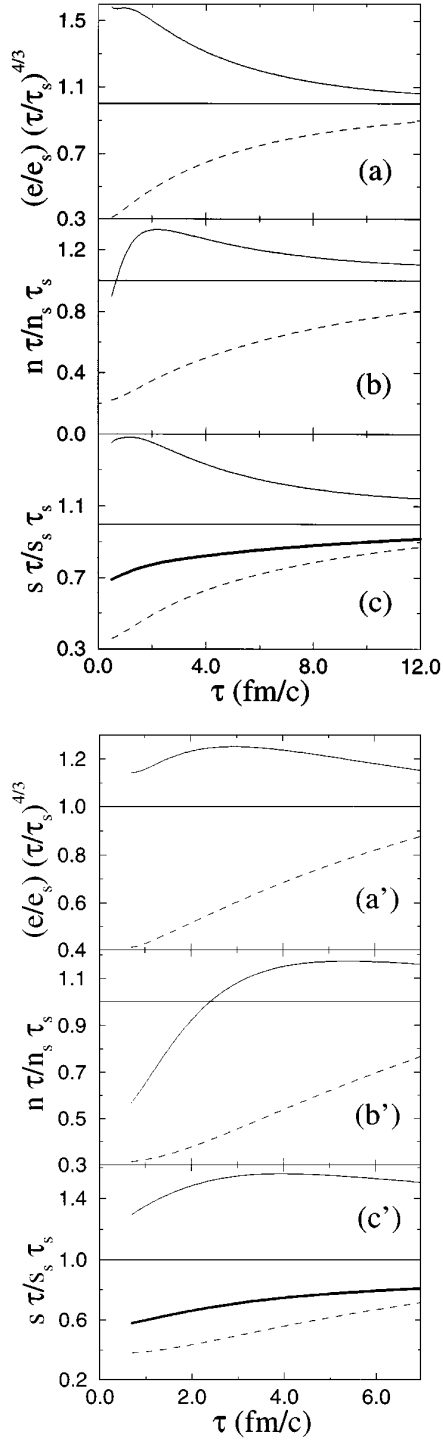
FIG. 3. The scaled products of the collective variables (a) energy density, (b) number density, and (c) entropy density and their expected inverse time dependence in equilibrium $\tau^{4/3}$, τ, and τ, respectively, at LHC. Graphs (a$'$), (b$'$), and (c$'$) are the same at RHIC. The solid and dashed lines are for gluons and quarks, respectively. The thick solid line in (c) and (c$'$) is the scaled product of the total entropy density and τ.

FIG. 4. The time dependence of the collision time (a) for gluons θ_g and (b) for quarks θ_q at LHC. Their values are compared in (c). τ overtakes first θ_g and later θ_q also. Graphs (a$'$), (b$'$), and (c$'$) are the same at RHIC. In this case, τ only has time to overtake θ_g but not θ_q.

sion entropy density rate is negative as shown in Fig. 6 and Fig. 7(c). We will see that this same interaction becomes dominant in the later part of the evolution later on when we compare the importance of the different processes. So gluons are losing energy, number and entropy to the fermions. This

has to be so before the system as a whole can settle into complete equilibrium. The thick solid lines in Fig. 3(c) and (c$'$) show the scaled total entropy per unit area in the central region which give an idea of the state of the system as a
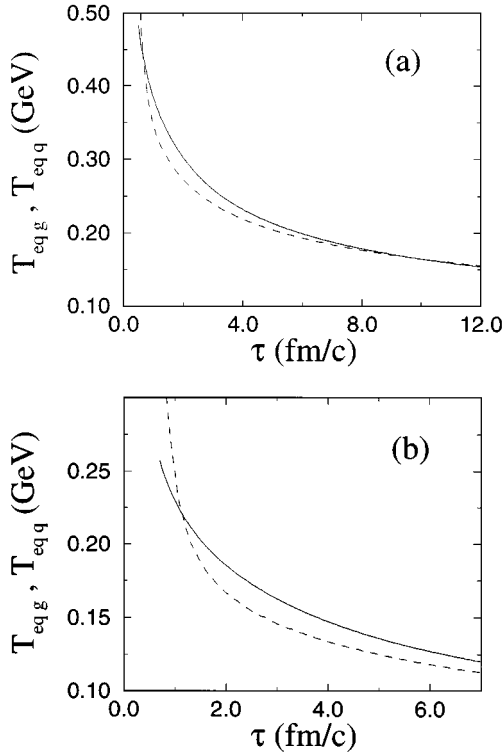
FIG. 5. The time development of the equilibrium target gluon (solid line) and quark (dashed line) temperatures T_{eqg} and T_{eqq}, respectively, at (a) LHC and (b) RHIC. They should converge in an oscillating fashion at large τ in order for the system to equilibrate as one towards a single temperature. The convergence is less good at RHIC than at LHC.

whole. They show that although the entropy of the individual subsystem can decrease, the total value must increase in accordance with the second law of thermodynamics.

The figures discussed above show that the plasma is indeed approaching equilibrium and that interactions are fast enough to dominate over the Bjorken type one-dimensional scaling expansion.

As we analyzed in Sec. III, thermalization is governed by the θ_i's. How fast this will proceed depends on their magni-

tudes and what is the actual final state depends on their time-dependent behaviors. For thermalization, the θ_i's must behave in such a way such that $x_i \rightarrow \infty$ as $\tau \rightarrow \infty$. That means they must grow less fast than τ. In Fig. 4, we show these θ_i's as a function of τ. Initially, $\theta_i > \tau$ for both quarks and gluons, and θ_q starts off very large (see Table I) but drops extremely rapidly back down to within hadronic timescales. The subsequent expected increase in time [36–38] is sufficiently slow for τ to get past θ_g and θ_q at LHC, Figs. 4(a) and (b) but at RHIC, Fig. 4(b'), θ_q is still too large for τ to overtake it before the temperature reaches 200 MeV. Nevertheless, the τ dependence is slow enough that x_i should go to infinity as $\tau \rightarrow \infty$.

We have mentioned in Sec. II, for the system to equilibrate as one, the target equilibrium temperatures T_{eqg} and T_{eqq} and also θ_g and θ_q must approach each other at large τ. We strongly suspect that the convergence of the temperatures will proceed in an oscillating fashion where the two curves intersect each other several times before the final convergence at very large τ. We can see this in Figs. 5(a) and (b). At LHC, the initial condition is more favorable for equilibration and so T_{eqg} intersects T_{eqq} twice already. This is not so at RHIC. In fact, all indications point to the fact that a plasma created at LHC will equilibrate better than one created at RHIC. By letting the plasma to continue its evolution and ignoring the deconfinement phase transition, we have seen that the collective variables like the gluon and quark energy densities, gluon entropy density, etc., do show tendency to pass from below to above or vice versa, the corresponding equilibrium target values, i.e., tendency to overshoot the equilibrium values and hence oscillation. As to the convergence of θ_i's, it is not so clear in Figs. 4(c) and (c'), especially at RHIC in Fig. 4(c'). θ_q is much too large in comparison with θ_g for any clear sign of convergence within the time available. On the other hand, at LHC, although there is still a large gap between the magnitudes, there is a clear tendency that the rate of increase of θ_q with τ is slowing down in Fig. 4(b) while θ_g still increases at approximately the same rate. It is simply too early for the system to equilibrate as one. Even near the end, the quarks and gluons can only be considered as two linked subsystems
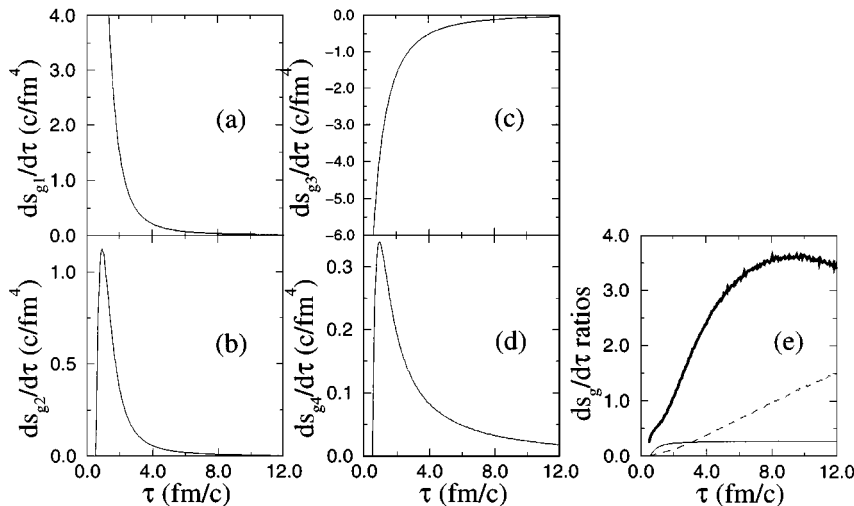

FIG. 6. The time development of the different contributions to the total gluon collision entropy density rate at LHC. They are (a) $gg \leftrightarrow ggg$, (b) $gg \leftrightarrow gg$, (c) $gg \leftrightarrow q\bar{q}$, and (d) $gq \leftrightarrow gq$ or $g\bar{q} \leftrightarrow g\bar{q}$. The curves of the elastic scattering processes in (b) and (d) have typical peaks at maximum anisotropy in momentum distributions. The ratios of the contribution (b) (thick line), (c) (solid line), and (d) (dashed line) to that of (a) are plotted in (e). This shows that first gluon multiplication dominates initially but is later overtaken by gluon annihilations into quark-antiquark pairs.
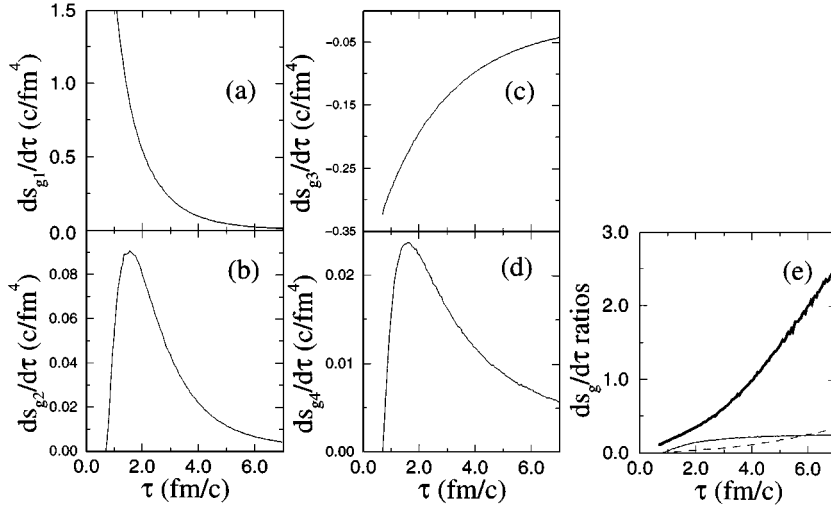
FIG. 7. The time development of the same contributions to the total gluon collision entropy density rate as in Fig. 6 but at RHIC. The same ratios between the different contributions as at LHC are plotted in (e).

approaching equilibrium at very different rates. Hence we have a two-stage equilibration.

Having shown that interactions can indeed dominate over the one-dimensional expansion of the parton gas in the central region of relativistic heavy ion collisions and hence bring the plasma into equilibrium. We can now look at the individual processes and compare their relative importance. These are the processes Eqs. (19), (20), and (21). We have labeled their contributions to the gluon and quark collision entropy rate $ds_g/d\tau$ and $ds_q/d\tau$ by $ds_{gi}/d\tau$, $i=1,\ldots,4$ and $ds_{qi}/d\tau$, $i=1,\ldots,3$ in the order that they appear in Eqs. (19), (20), and (21). Processes that give the same rate due to quark-antiquark symmetry are considered as the same process. Hence $gq \leftrightarrow gq$ and $g\bar{q} \leftrightarrow g\bar{q}$ give identical contribution to gluon and quark collision entropy density rate as $ds_{g4}/d\tau$ and $ds_{q2}/d\tau$, respectively. Also we have combined fermion elastic scattering processes as one rate $ds_{q3}/d\tau$ for convenience. These are shown in Fig. 6, Fig. 7, Fig. 8, and Fig. 9. The elastic processes have a characteristic shape, i.e., an initial rapid rise to a peak at maximum anisotropy before returning to zero progressively. The sharper the peak, the quicker the kinetic equilibration [compare Fig. 6 and Fig. 7(b), (d) and Fig. 8 and Fig. 9(b), (c) and Fig. 2]. Note the negative rate of Fig. 6 and Fig. 7(c) which is because there are net quark-antiquark pair creations from gluon-gluon annihilations and entropy decreases with the number of gluons as already mentioned in the previous paragraphs. We compare the different processes by plotting the ratio of the magnitude of each contribution to that of gluon multiplication for gluons in Fig. 6 and Fig. 7(e) and the ratio of each rate to that of quark-antiquark creation for quarks (antiquarks) in Fig. 8 and Fig. 9(d). In the (e) figures, gluon multiplication clearly dominates initially at $\tau \lesssim 2$ fm/c at LHC and $\tau \lesssim 4$ fm/c at RHIC since all three ratios in each plot are less than 1. After these times, $q\bar{q}$ creation becomes dominant (thick solid line) and rises to several times larger than gluon multiplication. The gg elastic scattering, on the other hand, tends to maintain a small, nearly constant ratio with gluon multiplication (solid line), which supports the claim made in [11]. That is, in a pure gluon plasma, gluon multiplication dominates over gg elastic scattering in driving the plasma towards equilibrium. This remains the case even when $l_g \sim 0.93$ which shows that this dominance is not sensitive to the value

of l_g. The remaining ratio of quark-gluon scattering to gluon multiplication continues to rise but not as rapidly as the first ratio. For quark entropy, Fig. 8 and Fig. 9(d), both ratios of quark-gluon scattering (solid line) and fermion-fermion scatterings (dashed line) to $gg \leftrightarrow q\bar{q}$ rate remain small during the time available although they are both on the rise. So for gluons, gluon multiplication dominates initially but is later overtaken by $gg \leftrightarrow q\bar{q}$ which continues to dominate over other elastic processes. For quarks (antiquarks), this same process dominates during the lifetime of the plasma.

These behaviors can be understood in the following way. Gluon branching dominates initially over any other processes so long as gluons are not near equilibrium. Once they approach saturation [the l_g estimates slow down their approach towards 1.0 in Figs. 1(a) and (b) at about the times mentioned above], gluon-gluon annihilation to quark-antiquark takes over as the dominant one because the fermions are still far from full equilibrium. Because of the latter reason, the other ratios involving quark or antiquark to gluon branching continue to rise.
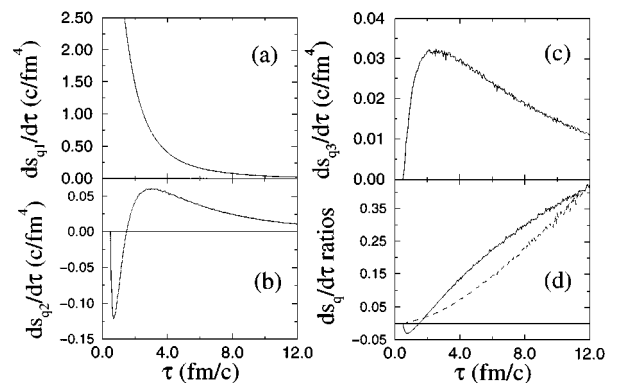

FIG. 8. The time development of the different contributions to the total quark collision entropy density rate at LHC. They are (a) $gg \leftrightarrow q\bar{q}$, (b) $gq \leftrightarrow gq$ or $g\bar{q} \leftrightarrow g\bar{q}$, and (c) the sum of the contributions of all fermion elastic scattering processes $qq \leftrightarrow qq$, $q\bar{q} \leftrightarrow q\bar{q}$, and $\bar{q}\bar{q} \leftrightarrow \bar{q}\bar{q}$. The ratios of the contribution (b) (solid line), (c) (dashed line) to that of (a) is plotted in (d). This shows that throughout the lifetime of the QCD plasma, gluon annihilations into quark-antiquark pairs dominates in the equilibration of the fermions.
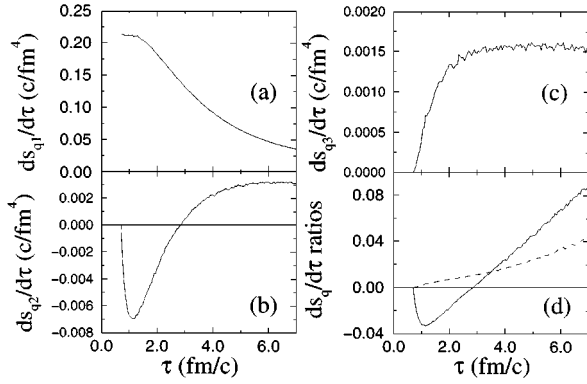
FIG. 9. The time development of the same contributions to the total quark collision entropy density rate as in Fig. 8 but at RHIC. The same ratios as at LHC are plotted in (d). They show again inelastic process dominates.

So contrary to common assumption, inelastic processes are dominant in equilibration. This should have consequences in the perturbative calculations of transport coefficients or relaxation times [36–38] of system that are not subjected to external forces. These calculations are based essentially, up to the present, on elastic binary interactions. As we have seen, they are not the dominant processes in equilibration.

To the surprising result of gluon multiplication dominates over elastic gluon-gluon scattering, we provide the following explanation. If one only looks at the scattering cross sections, it is indeed true that gluon-gluon scattering has a larger value and gluon multiplication processes are down by α_s for each extra gluon produced. The $(n-2)$ extra gluon production cross section can be expressed in terms of the elastic scattering cross section as [39,40], in the double logarithmic approximation,

$$\sigma_{gg\to(n-2)g} \propto \sigma_{gg\to gg}[\alpha_s \ln^2(s/s_{\text{cut}})]^{n-4}, \qquad (38)$$

where s_{cut} is the cutoff for the minimum binary invariant $(p_i+p_j)^2 > s_{\text{cut}}$ of the four-momenta of each gluon pair. In the present problem, $s_{\text{cut}} = m_D^2$, the double logarithm is not large and certainly does not compensate for the smallness of α_s. However, as we have mentioned at the beginning, the collision term on the rhs of Eq. (2) consists of the sum of the differences of the reactions in a QCD medium going forward and backward, so a large cross section does not automatically imply dominance of the corresponding process in the approach to equilibrium.

Similarly, $gg\leftrightarrow q\bar{q}$ is not that different from $gq\leftrightarrow gq$ or $g\bar{q}\leftrightarrow g\bar{q}$ because the two matrix elements are related simply by a swapping of the Mandelstam variables. So why should the first dominate over the second? Except the different ways that the infrared divergences are cut off in the processes, the main reason is $gg\to q\bar{q}$ dominates over the backward reaction $q\bar{q}\to gg$ due to the simple fact that there are less fermions than gluons present in the plasma. An extreme example of this phenomenon would be the forward and backward reaction balance out each other for all the elastic interactions as in a kinetically equilibrated plasma when only inelastic processes remain in the collision terms. In this extreme, all the ratios of elastic to inelastic collision entropy rate vanish.

We can now return to the question of whether other inelastic processes such as $gg\leftrightarrow q\bar{q}g$, $gq\leftrightarrow gqg$, $g\bar{q}\leftrightarrow g\bar{q}g$, $gq\leftrightarrow qq\bar{q}$, $g\bar{q}\leftrightarrow q\bar{q}\bar{q}$, $qq\leftrightarrow qqg$, etc., should be included. Although they are non-leading compared to $gg\leftrightarrow ggg$ and $gg\leftrightarrow q\bar{q}$ due to color, they should be significant when one sizes them with the elastic processes in view of the cancellation between the forward and backward reactions. In [11], the question of the dominance of inelastic over elastic processes was raised. Here it is sufficient to include the two leading inelastic processes to show this explicitly. Had one included these other processes, then equilibration should be faster and one could end up with a more reasonable quark-antiquark content in the plasma. However, we are doubtful that the equilibration time can be reduced dramatically from what we have shown here.

As we argued in [11], it is hard to perturb a parton system from thermal equilibrium without doing so chemically. Therefore inelastic processes are always active in the approach to equilibrium whereas the same is not true for elastic processes. From our figures, it can be seen that inelastic processes are not there only for chemical equilibrium or for minor contributions to thermalization as is commonly assumed due to their possible higher powers in α_s, they contribute even more significantly to equilibration than elastic processes. Changing the initial conditions will only vary the dominancy but not remove the dominance.

Before closing, we would like to point out some differences of our results with that of PCM. In PCM, there appears to be no early momentaneous isotropic particle momentum distribution in either S+S or Au+Au collisions. The first time that there is approximate isotropy, it is already thermalization according to [5]. It was claimed that there was no further significant change in the total momentum distribution after $\tau = 2.4$ fm/c for Au+Au collision at RHIC. We assume that they mean the shape of the distribution with the exception of the slope which should continue to change due to cooling. However, when the total distribution is broken down into that of the parton components, the approximate isotropy or thermalization becomes less obvious. We have shown that thermalization in the strict sense is slow and isotropy of gluon momentum distribution can be argued to be approximate but that of the fermions is not so good.

As to chemical equilibration, PCM shows little chance of that for the fermions. The corresponding fugacity estimates are approaching the "wrong direction" with increasing time. This is due to a net outflow of particles from the defined central region. The net flux of outgoing particles is arguably more important for fermions than for gluons because the formers have a larger mean free path. The result is the gluon (fermion) fraction of the particle composition rises (drops) with increasing time. Therefore even if there is no phase transition and the parton plasma is allowed to continue its one-dimensional expansion indefinitely, chemical equilibration will never be achieved. Then according to PCM, the expansion is slow enough for kinetic equilibration for all particle species but too fast for chemical equilibration of the quarks and antiquarks. The boundary effect is too important and is affecting equilibration. In our case, this effect is not incorporated. Although equilibration is slow, full equilibration will be reached given sufficient time.

We find it surprising that although the gluon fugacity estimate in PCM [6] overshoots and stays above or at 1.0 nearly all the time except at the beginning, R_g is still positive or an order of magnitude larger than $R_q + R_{\bar{q}}$ when the fugacities of the latter are well below 1.0 and decreasing. One would expect rather gluon absorption or conversion into quark-antiquark should take a significant toll on the gluon production so that there should be a diminution of gluons. At least, this should be the case when local kinetic equilibrium has been or nearly been reached which PCM claimed to be so at the end of the program run but this is not the case in the plot of the production rate of the different particle species. This is counterintuitive and opposite to what we have shown.

To conclude, we have shown that inelastic processes dominate in the approach towards equilibrium. In particular, gluon branching is most important. Gluon-gluon annihilation into quark-antiquark becomes more important only when the gluons are near saturation and equilibrium. The lower power in α_s of the gluon-gluon elastic scattering as compared to the inelastic gluon emission process is more than compensated

for by the cancellation of the reaction going forward and backward. The recovery of isotropy in momentum distribution is slow and so is chemical equilibration. The latter is partly due to the small initial fugacities that we used. As an intrinsic feature of perturbative QCD, the quarks and antiquarks are lagging behind the gluons in equilibration and hence a two-stage equilibration scenario.

ACKNOWLEDGEMENTS

[1] C.M. Hung and E.V. Shuryak, Phys. Rev. Lett. **75**, 4003 (1995).

[2] E.V. Shuryak, Phys. Rev. Lett. **68**, 3270 (1992).

[3] H. Heiselberg and X.N. Wang, Nucl. Phys. **B462**, 389 (1996).

[4] K. Geiger and B. Müller, Nucl. Phys. **B369**, 600 (1991).

[5] K. Geiger, Phys. Rev. D **46**, 4965, (1992); **46**, 4986 (1992).

[6] K. Geiger and J.I. Kapusta, Phys. Rev. D **47**, 4905 (1993).

[7] G. Baym, Phys. Lett. **138B**, 18 (1984).

[8] S. Gavin, Nucl. Phys. **B351**, 561 (1991).

[9] K. Kajantie and T. Matsui, Phys. Lett. **164B**, 373 (1985).

[10] H. Heiselberg and X.N. Wang, Phys. Rev. C **53**, 1892 (1996).

[11] S.M.H. Wong, Nucl. Phys. **A607**, 442 (1996).

[12] P. Danielewicz and M. Gyulassy, Phys. Rev. D **31**, 53 (1985).

[13] T.S. Biró, E. van Doorn, B. Müller, M.H. Thoma, and X.N. Wang, Phys. Rev. C **48**, 1275 (1993).

[14] P. Lévai, B. Müller, and X.N. Wang, Phys. Rev. C **51**, 3326 (1995).

[15] X.N. Wang, Nucl. Phys. **A590**, 47 (1995).

[16] J. Winter, J. Phys. (Paris) Colloq. **45**, C6-53 (1984).

[17] U. Heinz, Phys. Rev. Lett. **51**, 351 (1983).

[18] H.Th. Elze, M. Gyulassy and D. Vasak, Nucl. Phys. **B276**, 706 (1986); Phys. Lett. B **177**, 402 (1986).

[19] H.Th. Elze and U. Heinz, Phys. Rep. **183**, 81 (1989).

[20] H.Th. Elze, Z. Phys. C **47**, 647 (1990).

[21] H. Weigert and U. Heinz, Z. Phys. C **50**, 195 (1991).

[22] U. Heinz, in *Proceedings of the Banff/CAP Workshop on Thermal Field Theories*, edited by F.C. Khanna *et al.* (World Scientific Singapore, 1994), p. 428.

[23] S. de Groot, W.A. van Leuwen, and C.G. van Weert, *Relativistic Kinetic Theory*, (North-Holland, Amsterdam, 1980).

[24] G. Bertsch and J.F. Gunion, Phys. Rev. D **25**, 746 (1982).

[25] M. Gyulassy and X.N. Wang, Nucl. Phys. **B420**, 583 (1994).

[26] M. Gyulassy, M. Plümer, and X.N. Wang, Phys. Rev. D **51**, 3436 (1995).

[27] R. Baier, Yu.L. Dokshitser, S. Peigné, and D. Schiff, Phys. Lett. B **345**, 277 (1995).

[28] R. Cutler and D. Sivers, Phys. Rev. D **25**, 746 (1982).

[29] T.S. Biró, B. Müller, and X.N. Wang, Phys. Lett. B **283**, 171 (1992).

[30] K.J. Eskola, B. Müller, and X.N. Wang, Report No. HU-TFT-95-47, DUKE-TH-95-96, LBL-37642, hep-ph/9509285.

[31] E. Braaten and R.D. Pisarski, Nucl. Phys. **B337**, 569 (1990).

[32] J. Frenkel and J.C. Taylor, Nucl. Phys. **B334**, 199 (1990).

[33] A.H. Weldon, Phys. Rev. D **26**, 1394 (1982); **26**, 2789 (1982).

[34] V.V. Klimov, Yad. Fiz. **33**, 1734 (1981) [Sov. J. Nucl. Phys. **33**, 934 (1981)].

[35] J.C. Taylor and S.M.H. Wong, Nucl. Phys. **B346**, 115 (1990).

[36] G. Baym, H. Monien, C.J. Pethick, and D.G. Ravenhall, Nucl. Phys. **A525**, 415c (1991).

[37] G. Baym, H. Heiselberg, C.J. Pethick, and J. Popp, Nucl. Phys. **A544**, 569c (1992).

[38] H. Heiselberg, Phys. Rev. Lett. **72**, 3013 (1994).

[39] H. Goldberg and R. Rosenfeld, Phys. Lett. B **333**, 178 (1994).

[40] E.V. Shuryak and L. Xiong, Phys. Rev. C **49**, 2203 (1994).